Received: 24 March 2022 | Revised: 24 August 2022 | Accepted: 16 September 2022

IET Science, Measurement & Technology

DOI: 10.1049/smt2.12128

The Institution of Engineering and Technology WILEY

ORIGINAL RESEARCH

Investigation on combined effect of humidity–temperature on partial discharge through dielectric performance evaluation

Yatai Ji[1] | **Paolo Giangrande**[2] | **Weiduo Zhao**[1] | **Vincenzo Madonna**[3] | **He Zhang**[1] | **Jing Li**[1] | **Michael Galea**[4]

[1]Key Laboratory of More Electric Aircraft Technology of Zhejiang Province, University of Nottingham Ningbo China, Ningbo, China

[2]Department of Engineering and Applied Sciences, University of Bergamo, Dalmine (BG), Italy

[3]Advanced Engineering, PUNCH Torino S.p.A., Turin, Italy

[4]Department of Industrial Electrical Power Conversion, University of Malta, Msida, Malta

Correspondence
Weiduo Zhao, Key Laboratory of More Electric Aircraft Technology of Zhejiang Province, University of Nottingham Ningbo China, Ningbo 315100, China.
Email: zhaoweiduo@gmail.com

Funding information
National Key Research and Development Program of China, Grant/Award Number: 2021YFE0108600

Abstract

The humidity role in the partial discharge (PD) inception mechanism is quite challenging, especially when considering the environmental temperature. Indeed, there is no general rule to explain the humidity effect on the PD phenomenon. In this paper, the PD activity in inter-turn insulation is experimentally investigated for different relative humidity (RH) conditions at three different ambient temperatures, that is, 30°C, 60°C, and 90°C. Partial discharge inception voltage (PDIV) is directly measured through a photomultiplier tube (PMT), whereas the tip-up tests are performed aiming at monitoring both dissipation factor (tanδ) and insulation capacitance (IC). These extra measurements (diagnostic dielectric markers) allow better assessing the insulation status. The adoption of the tip-up test enables the insulation properties measurement. Based on the tip-up tests' findings, the interfacial polarization process starts at 75% RH under 60°C, while the high conductivity area is already formed at 75% RH when the ambient temperature is 90°C. The water film formation deduced from the tip-up test is then used to explain the trend of PDIV, and the validity is further proved by finite element analysis (FEA).

1 | INTRODUCTION

Partial discharge (PD) is a critical factor influencing the reliability of the insulation system, especially for Type I insulation. According to the International Electrotechnical Commission (IEC) standard [1], the occurrence of PD in Type I insulation (i.e. organic materials) means the end-of-life of the insulation system. Hence, PD activity should be avoided in electrical machines (EMs) insulated via Type I insulation. Environment factors including temperature, pressure, and humidity can influence PD activity. Paschen's law combined with finite element analysis (FEA) is used to interpret the pressure effect on PD [2]. Regarding the temperature impact, an increase in winding temperature from 25°C to 155°C typically leads to a fall of the partial discharge inception voltage (PDIV) by 30% as stated in the IEC standard [1]. However, there is no general rule which describes the humidity effect on the PD mechanism. The humidity effect on PD becomes critical considering EMs for offshore wind turbine application [3]. Moreover, for EMs with open ventilated cooling systems (low-cost and common cooling system solution), the moisture in the air can enter the housing and combined with the temperature generated by Joule effect creates a microclimate within the EM. Thus, it is important to fully analyse and investigate the PD inception mechanism under the combined action of both humidity and temperature.

1.1 | Literature review

Many publications have focused on the humidity effect on the PD phenomenon. The PD magnitude is measured for several relative humidity (RH) values in [4], and the insulation lifetime is predicted after PD occurrence. The obtained results indicate a higher PD magnitude along with a lifetime reduction at 90% RH. The trend of PDIV as a function of RH at fixed temperature levels is given in [5, 6], although the trends' explanation

is not provided. As discussed in [7], the trend of PDIV with RH is determined by the combined effect of the electric field enhancement caused by water film formation and the increased breakdown field of the air at high humidity levels. The dielectric response of insulation materials in a high humidity environment is investigated in [8, 9], but the correlation between the variation in dielectric properties and the PD inception mechanism is neglected.

In a comprehensive analysis, the temperature is an ambient factor to be accounted for when the insulation system for EM is assessed and several papers have been published regarding the combined effect of humidity and temperature on PDIV. In [10], the PDIV is detected at three RH levels considering three different ambient temperature values. Only PDIV and PD extinction voltage are measured, and the data are mainly used to quantify the percentage change in PDIV. Apart from PDIV measurement, optical emission spectroscopy is adopted to estimate the electric field strength in the air gap [11]. However, the variation of insulation properties caused by the high humidity environment is not evaluated. The relative permittivity and the hydrophilic property of the surface are determined by Kikuchi et al. [12], while the surface conductivity is calculated in [13]. In addition, the moisture content of the insulation film under different temperatures and RH levels is measured by a Karl Fisher moisture meter in [14]. These additional measurements help understand the PD inception mechanism through the change of insulation properties in different humidity environments. Nevertheless, the insulation status during the PD process under different RH conditions could not be measured. In other words, there is no direct relationship between the PD phenomenon and insulation status in a varying humidity environment.

1.2 | Research contribution

In this paper, a tip-up test of dissipation factor (tanδ) and insulation capacitance (IC) has been introduced for a better understanding of the PD inception mechanism. In fact, monitoring the dielectric properties while performing the PDIV test enables a comprehensive analysis of the phenomenon due to the simultaneous measurements.

The behaviour of a real dielectric material can be represented as a capacitor in parallel with a resistance. When the dielectric material is subjected to the sinusoidal voltage whose level is below the PDIV, the dielectric loss is mainly caused by the solid loss (i.e. conduction loss and polarization loss), which does not change much with the applied voltage. On the other hand, when the PD is incepted, there is a boost in the dielectric loss due to the rise in the ionization loss and thus the tanδ. The tanδ is the sum of tanδ_S, which accounts for the solid loss, and tanδ_{PD} which is linked to the ionization loss caused by PD, as shown in Figure 1 [15]. In addition, the inception of PD leads to a boost in IC, since the air voids between two conductors have been partially bridged [16]. Therefore, the tip-up test of tanδ and IC can be used as an indirect measurement of PD. In this paper, the PDIV has been measured at five different RH levels under three different ambient temperatures: 30°C, 60°C, and 90°C. Optical PD detection using a photomultiplier tube (PMT) is employed for direct PD measurement. Twisted pair is used as the test sample since it is a fair representation of turn-to-turn insulation and is easy to manufacture [17]. The tip-up test is carried out by industrial insulation tester Megger 4110. The tip-up test results sustain the water film condensation, which in turn explains the PDIV trend. The water film condensation is proved via the scanning electron microscope (SEM) images, whilst the PDIV trend is confirmed and validated through electrostatic FEA.

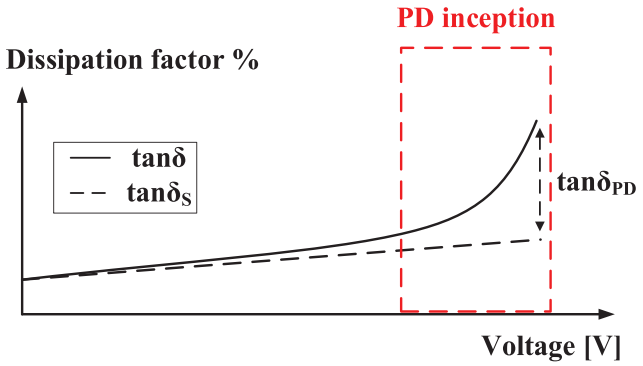

FIGURE 1 tanδ with increasing voltage [15]

TABLE 1 Insulation properties of enamelled magnet wire

Parameter	Property
Insulation material	Polyesterimide
Thermal class	H (180°C)
Wire diameter	0.63 mm
Insulation thickness	0.035 mm

2 | TEST SETUP AND PROCEDURE

2.1 | Specimen preparation

The premature failure of low-voltage EMs is commonly caused by excessive ageing and degradation of the turn-to-turn insulation [18]. Therefore, twisted pairs are chosen for the investigation. Such a configuration of specimens for studying humidity impact on PD is preferred referring to the literature [19–21]. In this paper, the enamelled magnet wires with the main properties listed in Table 1 are twisted following the IEC standard [22], as shown in Figure 2. The bare copper terminals at one end allow applying the excitation voltage. For each test condition, a set of five twisted pairs is employed for the statistical significance of the collected results. The test campaign is preceded by a preconditioning cycle [4, 20, 21], where the samples are wiped with alcohol to remove the unexpected contamination and then are exposed to a thermal treatment at 100°C for 1 h.

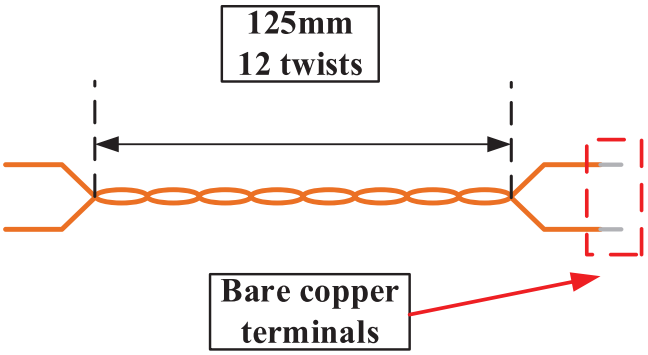

FIGURE 2 Configuration of twisted pair used for investigation

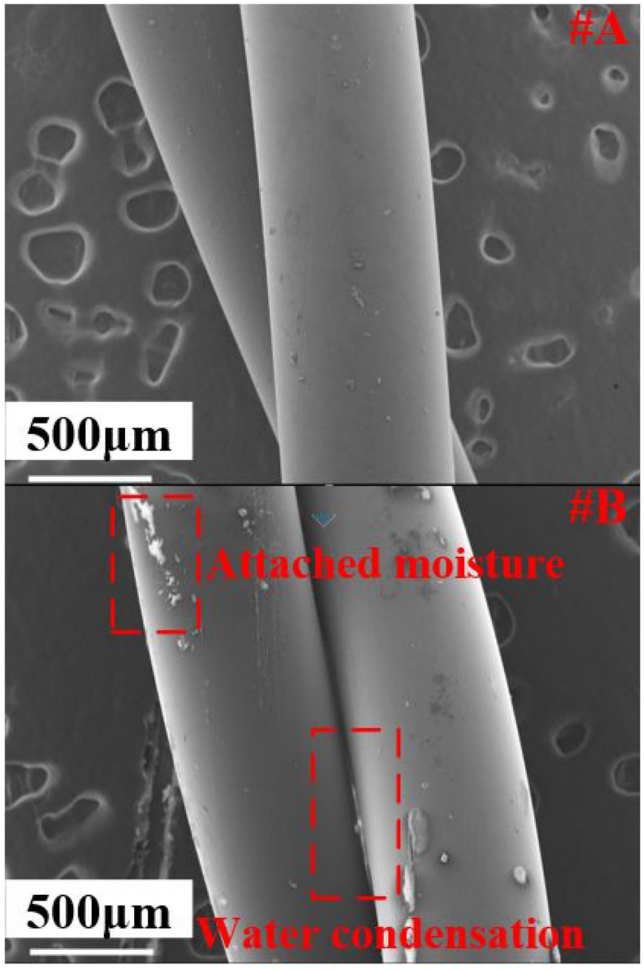

FIGURE 3 SEM micrograph of test samples. SEM, scanning electron microscope.

The morphology test via SEM is also carried out [23], with the purpose of evaluating the impact of humidity and temperature on the sample's surface. Figure 3 shows the SEM outcome, where Sample #A is a brand-new twisted pair after preconditioning, whereas sample #B experienced 2 h of exposure to high humidity and temperature environment (i.e. 90°C, 90% RH and 378 g/m^3 absolute humidity). The period of 2 h

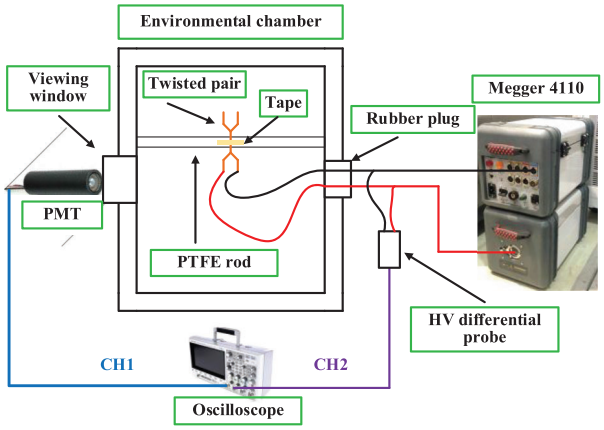

FIGURE 4 Scheme of the experimental test setup

corresponds to the typical time required to complete the whole investigation (i.e. PDIV measurement and tip-up test at five RH values and three temperature levels).

The SEM images indicate that (1) moisture could be attached to the insulation surface due to high humidity exposure and (2) water condensation is formed in the air gap between conductors. It is worthy to underline that the effect of water absorption due to long-term humidity is not considered in the present study.

2.2 | Experimental setup

The experimental setup employed for the investigation is schematized in Figure 4. A set of five specimens are hung to a Polytetrafluoroethylene (PTFE) rod fixed by an insulation tape and inserted inside the environmental chamber (ESPEC Co., type: ARS-0220) for accurate temperature and humidity adjustment. The rubber plug isolates the inside chamber from the outside environment while allowing pass-through of test leads. The tanδ and IC are measured by applying across the twisted pair insulation a 50-Hz sinusoidal voltage, whose amplitude is gradually increased from 0 to 700 Vrms. The excitation voltage generated by the Megger 4110 is also sensed via a high voltage (HV) differential probe and displayed on the KEYSIGHT® oscilloscope for convenience. The light emission associated with the PD inception is detected via the Hamamatsu® PMT, which is located outside the chamber window and its output is connected to the oscilloscope. In PD investigations under variable humidity conditions, the PMT represents a common choice for PD detection [11, 24, 25] because of its immunity to electromagnetic and acoustic interferences [26]. Black sheets covering the chamber window minimize and prevent the influence caused by excessive external light. In fact, the PMT is placed outside the chamber and in direct contact with the viewing window at approximately 30 cm from the twisted pairs. In Figure 5, the applied excitation voltage and the voltage signal (i.e. PTM output) associated with the PD are shown, as an example of PD direct measurement.

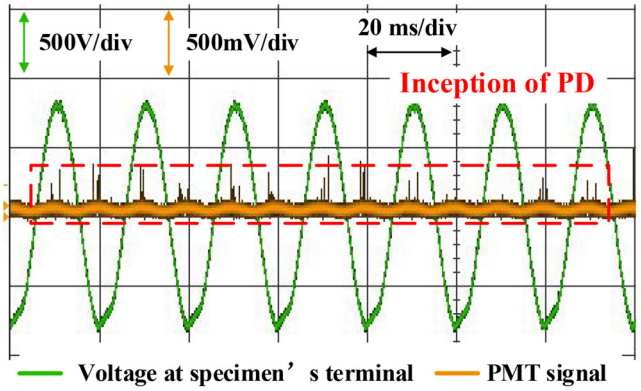

FIGURE 5 PMT voltage signals resulting from PD inception. PD, partial discharge; PMT, photomultiplier tube.

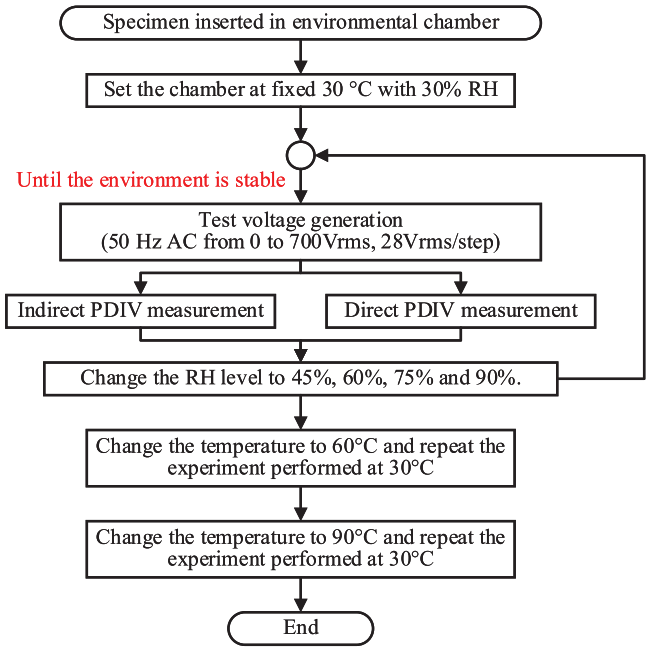

FIGURE 6 Flow diagram of the testing procedure

2.3 | Test procedure

The flow diagram of the testing procedure is illustrated in Figure 6. After the preconditioning treatment, a set of five twisted pairs is inserted inside the ESPEC chamber and a 30°C ambient temperature is set. Keeping constant the temperature throughout the test campaign, five RH values (i.e. 30%, 45%, 60%, 75%, and 90%) are considered. The significant number of tested humidity levels enables a clear overview of variability of tanδ, IC, and PDIV as a function of the humidity. Further, the selected RH values are compatible with the working conditions experienced by the EM insulation system operating in a high humidity environment (e.g. off-shore wind turbine).

Once the chamber reaches pre-set humidity and temperature values, the twisted pairs are excited with a sinusoidal voltage waveform. The Megger 4110 generates the auto-rising AC voltage from 0 to 700 V_{rms} with a 28 V_{rms} step (i.e. the minimum allowable step). At each step, the voltage holds for a few seconds for IC and tanδ measurements. At the same time, the PMT pointed at samples catches the light emitted by the PD inception, and the PDIV is registered. After the test at 30°C, a similar procedure is repeated using a new set of twisted pairs for the two remaining temperature values (i.e., 60°C and 90°C). In reality, it might not be possible to reach both high temperature and humidity values simultaneously (i.e. 90°C with 90% RH). Nevertheless, these test conditions aim at giving a comprehensive view of the PD phenomenon over a wide range of ambient parameters.

3 | EXPERIMENT RESULTS

The tanδ trend as a function of the excitation voltage for the examined ambient conditions is illustrated in Figure 7. At 30°C and 60°C (Figures 7a and 7b), when RH is within the range of 30% to 60%, there is no big difference in the tanδ measurements. The tanδ remains constant at a relatively low voltage level (up to 550 V_{rms}), and then it starts to increase steeply when PD is incepted. In Figure 7c, where the ambient temperature of 90°C is analysed, the trend just described holds for both 30% and 45% RH, while a different tendency is revealed at 60% RH. In particular, the tanδ linearly grows with the applied voltage until the PD is incepted causing a sudden step up in the tanδ value. When 75% RH is considered, the temperature plays a significant role in affecting the tanδ behaviour. At 30°C and 60°C, the tanδ features a rising trend with the applied voltage and a slight change of slope is still appreciable at relatively HV values (above 550 V_{rms}). Differently, the tanδ trend keeps increasing throughout the whole voltage range when the temperature is equal to 90°C and the change of slope (i.e. the point at which the PD is incepted) is not found. Assuming 700 V_{rms} as rated excitation voltage (U_N), the tanδ increment between 0.2 × U_N (i.e. 140 V_{rms}) and 0.6 × U_N (i.e. 420 V_{rms}) is calculated ($\Delta\tan\delta_{(420\text{-}140)}$) and listed in Table 2. An observable change in the $\Delta\tan\delta_{(420\text{-}140)}$ occurs at 75% RH and 60% RH at 60°C and 90°C ambient temperature, respectively. Additionally, the slope of the tanδ (or $\Delta\tan\delta_{(420\text{-}140)}$) boosts at 75% RH for higher temperatures. Finally, the samples exhibit the same dielectric performance regardless of the ambient temperature at 90% RH, (i.e. the tanδ increases linearly with the excitation voltage), and the recorded tanδ grows with the temperature.

For the sake of clarity, the tanδ at 0.6 × U_N is plotted for different RH–temperature combinations, as reported in Figure 8. The 0.6 × U_N is selected because PD is not incepted, but a significant tanδ is detectable. In general, it can be seen that the tanδ grows with the RH for the three temperature levels. However, the increasing rate becomes notable when the RH reaches 75% at both 30°C and 60°C temperatures, whereas an important increasing rate is already appreciable at 60% RH for 90°C ambient temperature. In addition, at the higher temperature, the value of tanδ is more influenced by the change of RH.

Figure 9 presents the trend of IC as a function of the RH for the three temperature levels. Below 60% RH, the IC does

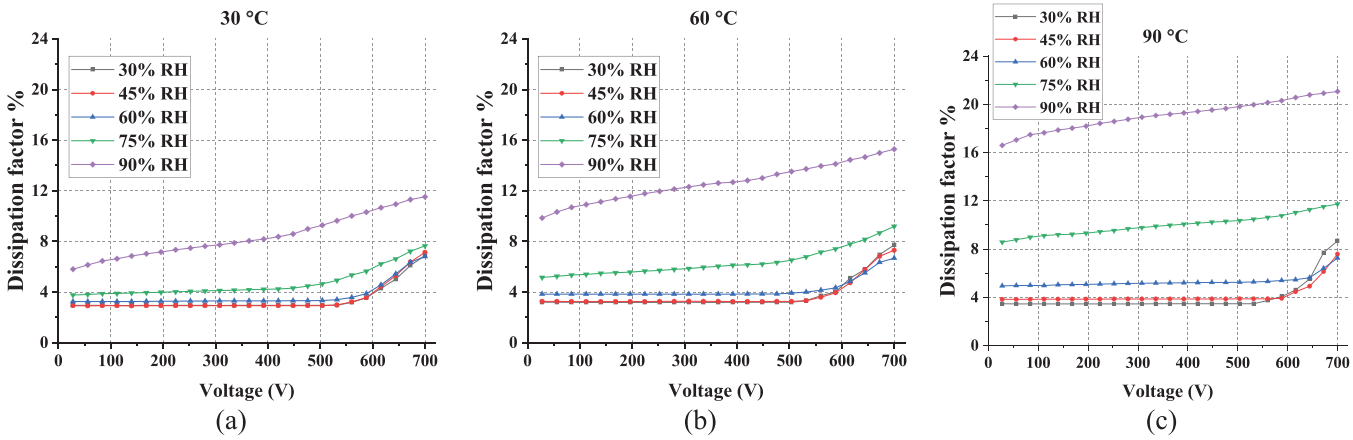

FIGURE 7 tanδ with applied voltage at different RH/temperatures. RH, relative humidity.

TABLE 2 % $\Delta\tan\delta_{(420\text{-}140)}$ at different temperature/RH

Temperature°C	RH %	% $\Delta\tan\delta_{(420\text{-}140)}$
30	45	0.01324
	60	0.04886
	75	0.32185
60	45	0.00538
	60	0.00782
	75	0.69183
90	45	0.02014
	60	0.1786
	75	0.94906

not experience relevant changes due to the different ambient temperatures. At 30°C and 60°C, differences in the IC measurements are noticeable when the RH reaches 90%, while significant variations in the IC values are evident at lower RH, that is, 75%, when the ambient temperature is 90°C.

Analyzed the tanδ and the IC, attention is given to the PDIV values directly measured via PMT. The PDIV trend with RH for different temperature levels is given in Figure 10. In general, the PDIV monotonically increases with the RH and higher PDIV values are detected at greater temperatures. A closer look at Figure 10 highlights that for 30°C and 60°C, the PDIV is not heavily affected if the RH is within the range from 30% to 60%. The PDIV increment expressed in V_{rms} for the value detected at 45% RH is summarized in Table 3 (PDIV at 30% RH could be considered a relatively low humidity value and it can be discarded). A boost of PDIV is found at 90% RH and 75% RH for 30°C and 60°C ambient temperatures respectively. Conversely, the PDIV trend is almost linear at 90°C.

Finally, absolute humidity is also considered and the PDIV values are plotted against the absolute humidity values in Figure 11. The PDIV is strictly increasing with the absolute humidity and small increments of absolute humidity result in higher PDIV for lower ambient temperatures. Further, a higher

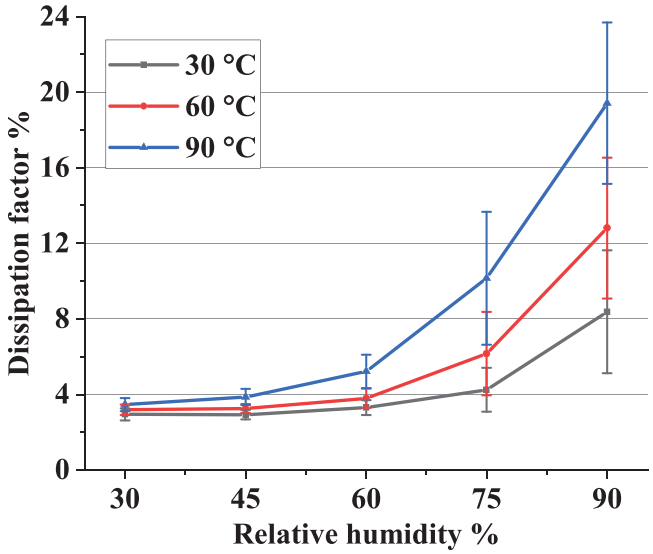

FIGURE 8 tanδ at 0.6 U_N at different RH/temperatures

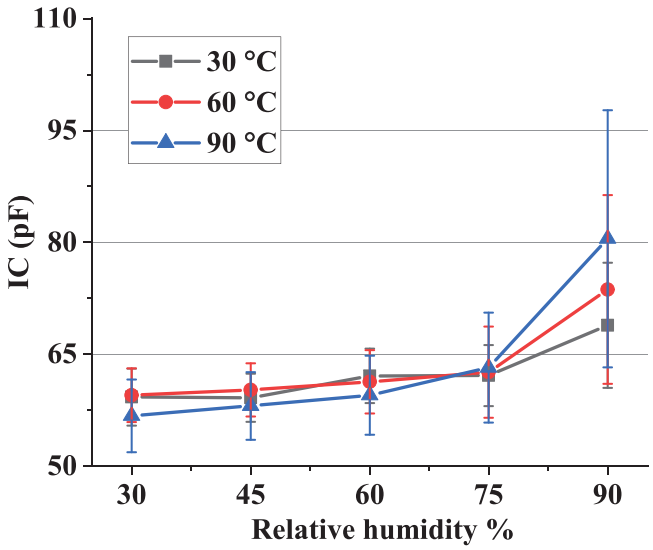

FIGURE 9 IC at 0.6 U_N at different RH/temperatures. IC, insulation capacitance.

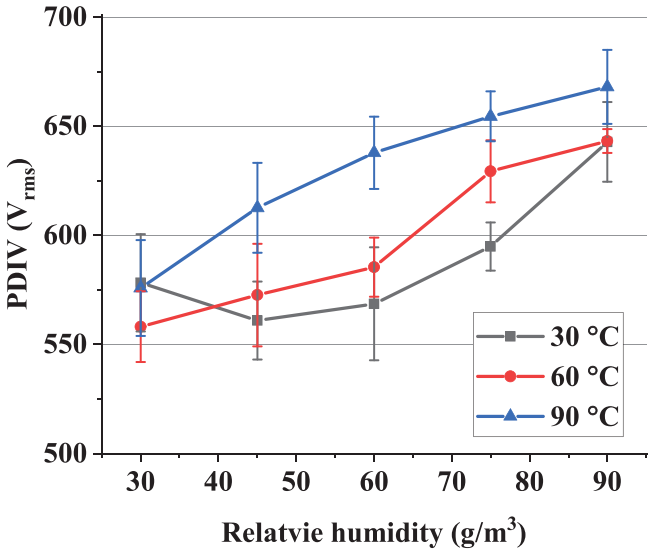

FIGURE 10 Trend of directly measured PDIV with RH at three different ambient temperature. PDIV, partial discharge inception voltage.

TABLE 3 Increment of PDIV in V_{rms}

Temperature°C	RH %	ΔPDIV (V_{rms})
30	60	7.66
	75	33.88
	90	81.78667
60	60	12.76667
	75	56.72667
	90	70.61667
90	60	25.2
	75	41.86
	90	55.36

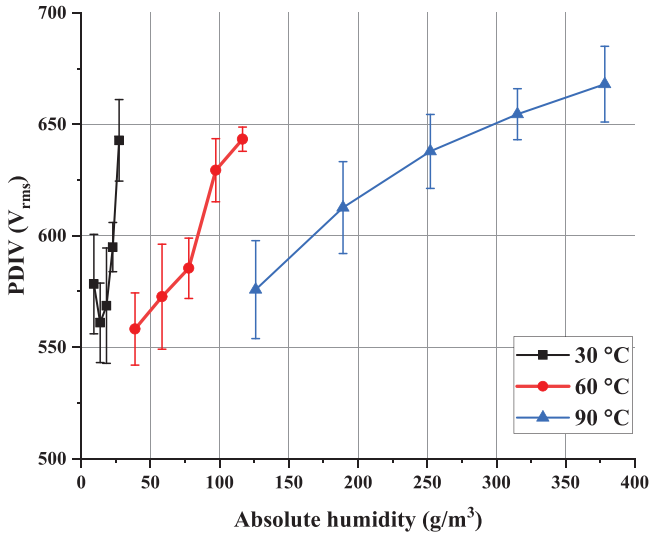

FIGURE 11 Trend of PDIV with absolute humidity

temperature leads to a decrease in PDIV, although absolute humidity keeps increasing.

4 | RESULTS DISCUSSION

4.1 | Deduction of water film condensation from tip-up test

The combined effect of humidity and temperature on the tanδ could be better explained by introducing the concept of water film condensation. At different temperature levels, three different conditions can be identified depending on RH, as depicted in Figure 12. At the lower RH level, there is no water film condensation due to the relatively low availability of water molecules in the atmosphere. The water film builds up on the insulation surface at medium RH levels, but only a limited portion of the surface is covered by it (i.e. the superficial path still features a low conductivity with the tendency towards higher conductivity values). At this stage, the slight tanδ increment with the applied voltage is mainly due to loss caused by the interfacial polarization, which is derived from the large difference in conductivities and permittivities between two adjacent layers (i.e. water film and polyesterimide film). At a higher RH level, the water film fills the gap between two conductors and a conduction path is formed leading to a boost in tanδ.

Considering the water film condensation, the results presented in Figure 7 are accordingly organized as listed in Table 4. When the temperature is equal to 90°C, the water film forms at 60% RH, while its formation occurs at 75% RH in the case of 30°C and 60°C. Therefore, at the highest temperature, that is, 90°C, the water film builds at a lower RH value compared to the other two temperatures examined.

The introduced explanation is also supported by the findings in Figure 9. When the water film is not yet formed or does not reach the contact point, there is no big difference in the IC measurements. On the contrary, the IC boosts if the water film fills the gap between two turns (i.e. 'shorted out' air voids). Therefore, the collected results allow concluding that temperature and absolute humidity do not play a major role in the dielectric diagnostic markers (tanδ and IC) until the water film is formed.

4.2 | Effect of water film condensation on PDIV

In this section, the water film condensation deduced from the tip-up test results is exploited for explaining the combined effect of RH and temperature on the PDIV. At 30°C, when the water film is not formed yet, the PDIV value does not change much if the RH is included in the range from 30% to 60%. Conversely, within the same RH range (i.e. 30%–60%), a boost in ambient temperature (from 30°C to 60°C) leads to a slight rise in the detected PDIV values.

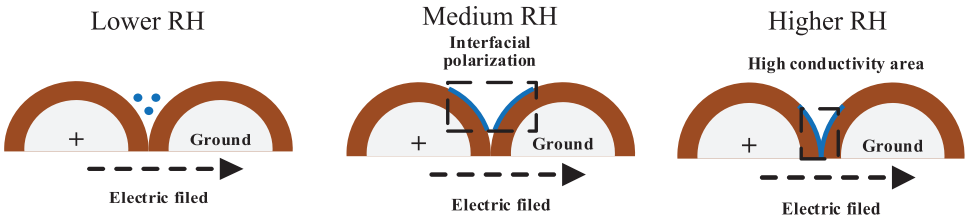

FIGURE 12 The humidity effect on twisted pairs

TABLE 4 The RH range definition at different ambient temperatures

Temperature (°C)	30	60°	90°
Lower RH range (%) (no water film formation)	30–60	30–60	30–45
Medium RH (%) (interfacial polarization exists)	75	75	60
Higher RH (%) (high conductivity area exists)	90	90	75–90

Finally, a further step-up in the ambient temperature (from 60°C to 90°C) results in a significant amplification of the recorded PDIV values. The PDIV growth with temperature can be attributed to the higher absolute humidity available in the test environment. When the RH passes from 30% to 60%, the corresponding absolute humidity varies from 9.09 to 18.19 g/m^3 if the temperature of 30°C is considered. At 60°C, the same interval of RH (i.e. 30%–60%) results in a change of absolute humidity from 38.86 to 77.72 g/m^3. Such a variation is further enhanced in the case of 90°C, where the absolute humidity goes from 126.11 to 252.22 g/m3. In other words, the same RH range (i.e. 30%–60%) will result in a massive rise in terms of absolute humidity as the temperature increases. Therefore, the availability of water vapour is greater at higher temperatures. However, vapour acts like an electro-negative gas increasing the electrical breakdown strength of the atmospheric air [7]. Thus, higher vapour contents (i.e. significant absolute humidity levels) due to the warmer ambient will cause an increment in PDIV.

The boost in PDIV values might be due to the consistent leakage current promoted by the water film formation and the consequent distortion of the resultant electric field. To support this explanation, the electric field distribution at several water film thicknesses is examined via electrostatic FE simulations in the next subsection.

Considering a given ambient temperature, the collected results allow stating that both RH and absolute humidity affect the PDIV. Indeed, the water film formation is ruled by the RH, while the absolute humidity plays its influence on the availability of the electro-negative gas (i.e. water vapour).

The comparison among different temperature levels makes the analysis more challenging because both humidity and temperature may affect the PDIV. Despite the challenge, four points exempt from water film condensation are selected to highlight the combined effect of temperature and absolute humidity on PDIV. The absence of water film condensation avoids the electric field distortion. In Table 5, the chosen points are detailed and by comparing the pair of points A-B and C-D, the

TABLE 5 The environmental conditions and corresponding PDIV values of four selected points

	Temperature (°C)	Relative humidity	Absolute humidity (g/m^3)	PDIV (V_{rms})
A	30	60%	18.19	568.64
B	60	30%	38.86	558.17
C	60	60%	77.72	585.40
D	90	30%	126.11	575.84

PDIV decreases although the absolute humidity keeps increasing. This finding is reasonable since the increasing temperature will decrease the PDIV. Hence, in the absence of water film condensation, the temperature effect dominates the PDIV value although the absolute humidity must be taken into account. Indeed, points B and D feature the same RH, but the PDIV of point D is greater despite its higher temperature due to considerable absolute humidity.

4.3 | Validation of water film influence on PDIV through electrostatic FE simulations

Aiming at confirming the PDIV measurements and validating the electric field distortion caused by the presence of the water film, electrostatic finite element (FE) simulations are performed. Such a method is commonly used for PD phenomenon prediction and explanation [27, 28]. The FE model consists of two turns and a variable thickness of water film

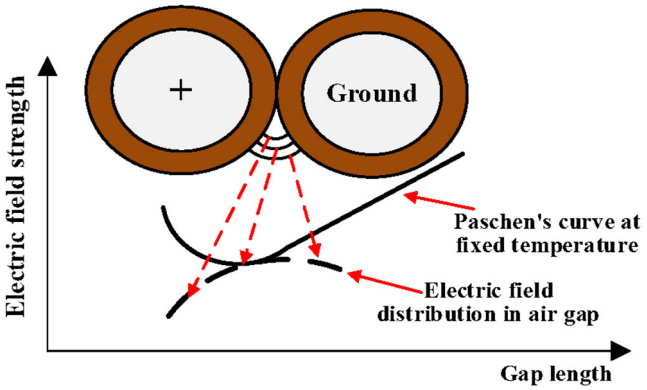

FIGURE 13 PDIV modelling based on Paschen's curve

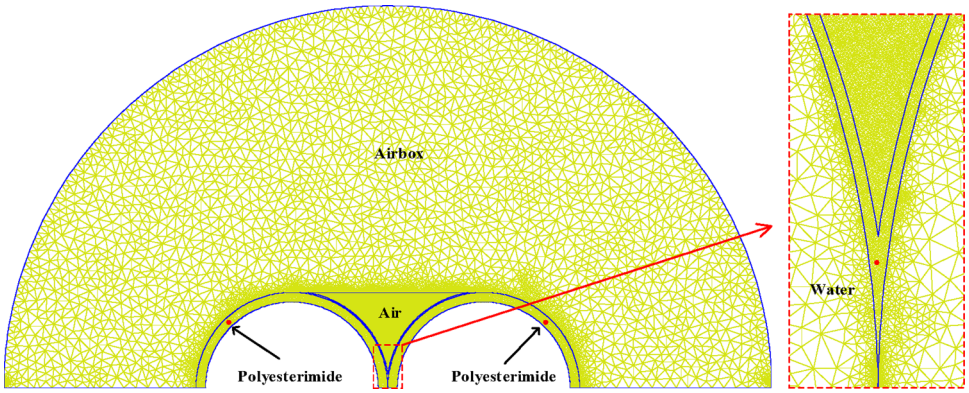

FIGURE 14 Mesh setup of the electrostatic FE simulation. FE, finite element.

TABLE 6 FE model: mesh definition and material properties

	Mesh size	Relative permittivity
Polyesterimide	0.01	3.4
Water film	0.001	76.75
Air	0.001	1
Airbox	0.1	1

surrounding the wire. The inter-turn electric field is calculated, while the PDIV value is determined through Paschen's law [29]. In particular, the voltage level assumed as the PDIV value from the FE simulations is obtained from the intersection between Paschen's curve at a given temperature and the electric field distribution in the air gap. A schematic illustration of how the PDIV value is determined using Paschen's law is shown in Figure 13. The software FEMM is adopted to simulate the electric field distribution between the two turns. Since accurate data on the water film thickness under different humidity conditions is not currently available in the literature, it is fair to assume 2 and 4 μm as reasonable thickness values. The mesh setup of the FE model is presented in Figure 14 with the main parameters listed in Table 6. The electric field distribution corresponding to these conditions is illustrated in Figure 15.

The temperature effect is taken into account via the Dunbar correction [30]. The relationship between pressure and temperature could be linked by the ideal gas law

$$pV = Nk_BT \tag{1}$$

where V is the volume of the ideal gas, N is the number of particles, and k_b is the Boltzmann constant. Thus, the equivalent pressure considering the temperature correlation can be expressed as

$$p_n = p_i \times \frac{T_i}{T_n} \tag{2}$$

where p_i and T_i are pressure and temperature at the initial temperature level, while p_n and T_n are the related values at the new temperatures. For the temperatures considered in the experimental investigation (i.e. 30°C, 60°C, and 90°C), the Paschen's curve is determined through the Dunbar corrections. These curves are reported in Figure 16 (continuous lines), together with the electric field distribution (dashed lines) at different water film thicknesses. The PDIV value obtained from FE simulations when no water film surrounds the wire surface (i.e. 0 μm thickness) is equal to 820.24 V_{Peak} (i.e. 580 Vrms). This value is close to the PDIV measured at 30°C and low RH level (i.e. 578.3 Vrms at 30% RH). The red shaded area in Figure 16 represents the high PD risk region, where the PD is most likely to be incepted. In this area, the required breakdown field decreases with the increase in temperature, while the electric field is reduced by the increment of water film thickness. In Figure 7c, considerable tanδ values are observed as the RH raises. Thus, the assumption of considering the formation of a thicker water film is reasonable and explains the PDIV experimental trend, although the actual thickness of the water film is unknown (i.e. the higher temperature reduces the required breakdown electric field strength, but boosts the actual electric field in the air gap caused by thicker water film). It is important to note that Paschen's law does not account for the effect of water vapour as an electro-negative gas, which further boosts the breakdown electric field. Hence, the trend of PDIV with RH at 90°C (before the water film formation) cannot be simply explained through Paschen's law, and further research to determine an appropriate correction factor is required.

5 | CONCLUSION

The inter-turn PDIV behaviour under sinusoidal voltage excitation was experimentally investigated considering the influence of both temperature and RH. Dielectric diagnostic markers, such as tanδ and IC, were employed for monitoring the insulation status and their measurements supported the idea of water film formation on the insulation surface. The effect of water film condensation on the electric field distribution was verified via electrostatic FE simulations and the corresponding outcomes confirmed the assumption validity. Therefore, the experimental PDIV trend was explained relying on the water

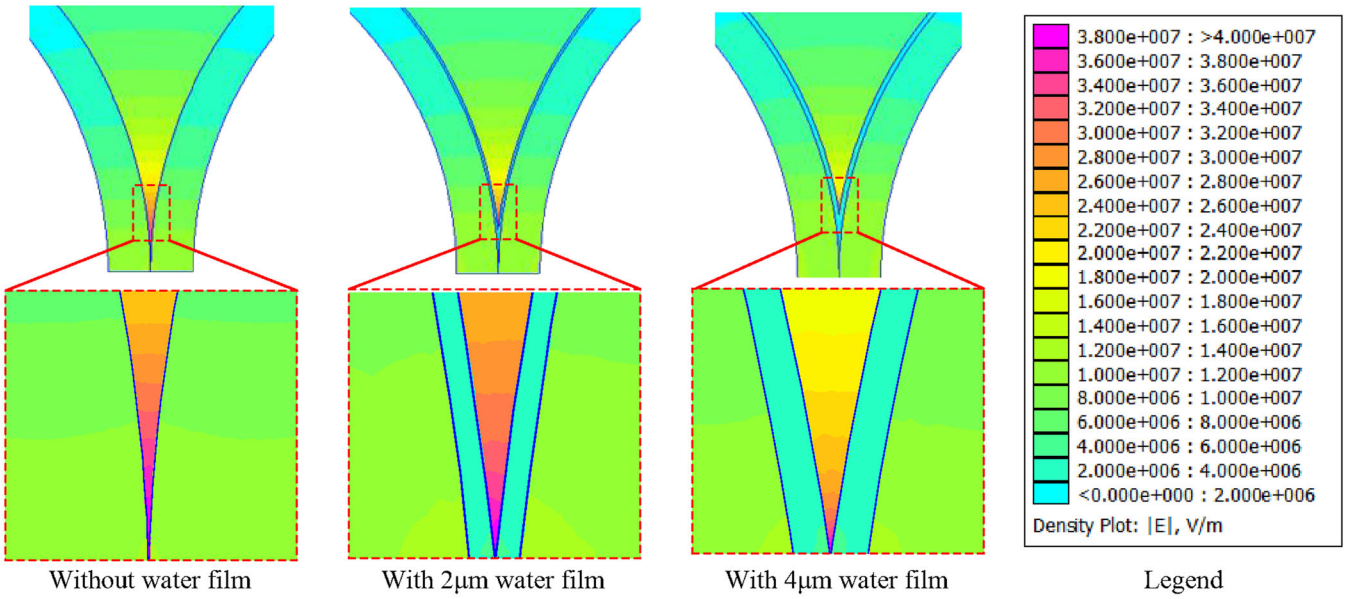

FIGURE 15 FE simulation results for 0.63 mm GR2 wire and V_{peak} = 820 V

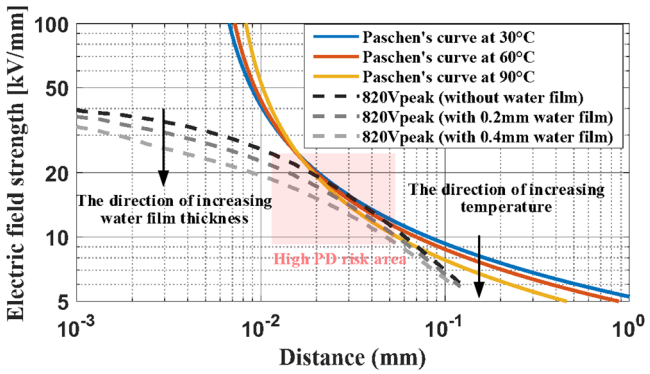

FIGURE 16 Electric field distribution for 0.63 mm and GR2 wire

film condensation for the examined ambient conditions. Based on the experimental findings, the following conclusions can be drawn:

1. The dielectric properties (i.e. tanδ and IC) are heavily influenced by the water film formation. Such behaviour was detected at all the considered temperatures, although the RH value at which the water film builds up changes with the ambient temperature (i.e. the water film formed at 75% under 60°C, while at 60% RH when the temperature is 90°C).
2. At a fixed temperature, the RH determines the water film formation, while the absolute humidity affects the water vapour availability. Both factors boost the PDIV.
3. The PDIV decreases with temperature, but the absolute humidity should be also considered because the PDIV at 60°C and 77.72 g/m^3 absolute humidity (i.e. 585.4 V_{rms}) is higher than the value at 30°C and 18.19 g/m^3 absolute humidity (i.e. 568.65 V_{rms}).

In the performed investigation, PD and dielectric diagnostic measurements were integrated aiming at providing a comprehensive explanation for a complex phenomenon. This approach proved the tip-up test as an effective tool for understanding the physics of PD under combined temperature–humidity conditions. In the future, a similar methodology can be used for investigating the PDIV of thermally aged and/or impregnated samples exposed to humidity conditions.

AUTHOR CONTRIBUTIONS

Yatai Ji: Conceptualization, data curation, formal analysis, investigation, methodology, validation, writing original draft. Paolo Giangrande: Conceptualization, investigation, methodology, visualization, writing – review & editing. Weiduo Zhao: Project administration, supervision, writing – review & editing. Vincenzo Madonna: Conceptualization, methodology, writing – review & editing. Jing Li: Resources, writing – review & editing. He Zhang: Funding acquisition, writing – review & editing. Michael Galea: Project administration, supervision, writing – review & editing.

ACKNOWLEDGEMENTS

This work is supported by Ministry of Science & Technology under National Key R&D Program of China, under Grant 2021YFE0108600.

CONFLICT OF INTEREST

The authors declare no conflict of interest.

FUNDING INFORMATION

This work is supported by Ministry of Science & Technology under National Key R&D Program of China, under Grant 2021YFE0108600.

DATA AVAILABILITY STATEMENT

The data that support the findings of this study are available from the corresponding author upon reasonable request. The data are not publicly available due to privacy restrictions.

REFERENCES

1. IEC 60034: Part 18–41: Partial Discharge Free Electrical Insulation Systems (Type I) Used in Rotating Electrical Machines Fed from Voltage Converters—Qualification and Quality Control Tests. (2014)
2. Madonna, V., Giangrande, P., Zhao, W., Zhang, H., Gerada, C., Galea, M.: Electrical machines for the more electric aircraft: Partial discharges investigation. IEEE Trans. Ind. Appl. 57(2), 1389–1398 (2020)
3. Malliou, C.-P., Karlis, A.D., Danikas, M.G., Lloyd, B.: A short review on the offshore wind turbine generator windings' insulation and the effect of water droplets and salinity. IEEE Trans. Ind. Appl. 52(6), 4610–4618 (2016)
4. Wang, P., Gu, Y., Wu, Q., Cavallini, A., Zhang, Q., Zhang, J., Li, P., Li, Y.: Influence of ambient humidity on PDIV and endurance of inverter-fed motor insulation. In: IEEE Electrical Insulation Conference (EIC), IEEE (2009)
5. Lusuardi, L., Rumi, A., Cavallini, A., Wang, P., Han, T.: Can low voltage inverter-fed induction motors be designed allowing partial discharge activity? In: IEEE Electrical Insulation Conference (EIC), IEEE (2009)
6. Kikuchi, Y., Ishida, T., Ueno, T., Kanazawa, S., Nagao, M., Hikita, M., Murakami, Y., Nagata, M.: Recent progress in round-robin test of repetitive partial discharge inception voltage measurements on complete winding of 4 Kw random-wound motor. In: 2017 International Symposium on Electrical Insulating Materials (ISEIM) (2017)
7. Fenger, M., Stone, G.C.: Investigations into the effect of humidity on stator winding partial discharges. IEEE Trans. Dielectr. Electr. Insul. 12(2), 341–346 (2005)
8. Soltani, R., David, E., Lamarre, L.: Impact of humidity on dielectric response of rotating machines insulation system. IEEE Trans. Dielectr. Electr. Insul. 17(5), 1479–1488 (2010)
9. Küchler, F., Färber, R., Franck, C.M.: Humidity and temperature effects on the dielectric properties of pet film. In: IEEE Electrical Insulation Conference (EIC), (2020)
10. Driendl, N., Pauli, F., Hameyer, K.: Influence of ambient conditions on the qualification tests of the interturn insulation in low-voltage electrical machines. IEEE Trans. Ind. Electron. 69(8), 7807–7816 (2021)
11. Kikuchi, Y., Murata, T., Fukumoto, N., Nagata, M., Wakimoto, Y., Yoshimitsu, T.: Investigation of partial discharge with twisted enameled wires in atmospheric humid air by optical emission spectroscopy. IEEE Trans. Dielectr. Electr. Insul. 17(3), 839–845 (2010)
12. Kikuchi, Y., Murata, T., Uozumi, Y., Fukumoto, N., Nagata, M., Wakimoto, Y., Yoshimitsu, T.: Effects of ambient humidity and temperature on partial discharge characteristics of conventional and nanocomposite enameled magnet wires. IEEE Trans. Dielectr. Electr. Insul. 15(6), 1617–1625 (2008)
13. Rumi, A., Cavallini, A., Lusuardi, L.: Combined effects of temperature and humidity on the Pdiv of twisted pairs. In: 2020 IEEE 3rd International Conference on Dielectrics (ICD) (2020)
14. Kaji, T., Asai, H., Kojima, H., Hayakawa, N.: Combined effect of temperature and humidity of magnet-wires on partial discharge inception voltage under inverter-surge voltage. In: 2018 IEEE Conference on Electrical Insulation and Dielectric Phenomena (CEIDP) (2018)
15. Madonna, V., Giangrande, P., Galea, M.: Evaluation of strand-to-strand capacitance and dissipation factor in thermally aged enamelled coils for low-voltage electrical machines. IET Sci. Meas. Technol. 13(8), 1170–1177 (2019)
16. Stone, G.C., Boulter, E.A., Culbert, I., Dhirani, H., Electrical Insulation for Rotating Machines: Design, Evaluation, Aging, Testing, and Repair. John Wiley & Sons, New York (2004)
17. Naderiallaf, H., Giangrande, P., Galea, M.: A contribution to thermal ageing assessment of glass fibre insulated wire based on partial discharges activity. IEEE Access 10, 41186–41200 (2022)
18. Galea, M., Giangrande, P., Madonna, V., Buticchi, G.: Reliability-oriented design of electrical machines: The design process for machines' insulation systems must evolve. IEEE Ind. Electron. Mag. 14(1), 20–28 (2020)
19. Busch, R., Pohlmann, F., Muller, K.: The influence of several environmental conditions on the partial discharge characteristics and on the lifetime of magnet wires under inverter pulse operation. In: Proceedings of 2001 International Symposium on Electrical Insulating Materials (ISEIM). 2001 Asian Conference on Electrical Insulating Diagnosis (ACEID 2001). 33rd Symposium on Electrical and Electron. Insulating Materials and Applications in Systems (2001)
20. Fenger, M., Campbell, S.R., Pedersen, J.: Motor winding problems caused by inverter drives. IEEE Ind. Appl. Mag. 9(4), 22–31 (2003)
21. Kimura, K., Hikita, M., Hayakawa, N., Nagata, M., Kadowaki, K., Murakami, Y.: Round-robin test on repetitive pd inception voltage of twisted-pairs. In: Annual Report Conference Electrical Insulation and Dielectic Phenomena (CEIDP) (2010)
22. IEC 60851: Winding Wires - Test Methods - Part 5: Electrical Properties. (2008)
23. Abdel-Gawad, N.M., El Dein, A.Z., Mansour, D.E.A., Ahmed, H.M., Darwish, M.M., Lehtonen, M.: PVC nanocomposites for cable insulation with enhanced dielectric properties, partial discharge resistance and mechanical performance. High Voltage. 5(4), 463–471 (2020)
24. Rokunohe, T., Kato, T., Kojima, H., Hayakawa, N., Okubo, H.: Calculation model for predicting partial-discharge inception voltage in a non-uniform air gap while considering the effect of humidity. IEEE Trans. Dielectr. Electr. Insul. 24(2), 1123–1130 (2017)
25. Kikuchi, Y., Murata, T., Uozumi, Y., Fukumoto, N., Nagata, M., Wakimoto, Y., Yoshimitsu, T.: Considerations on partial discharge of nanocomposite enameled magnet wires for inverter fed random wound motors. In: International Symposium on Electrical Insulating Materials (ISEIM 2008), IEEE (2008)
26. Schwarz, R., Muhr, M.: Modern technologies in optical partial discharge detection. In: Annual Report-Conference on Electrical Insulation and Dielectric Phenomena, IEEE (2007)
27. Abdel-Gawad, N.M., El Dein, A.Z., Mansour, D.E.A., Ahmed, H.M., Darwish, M.M., Lehtonen, M.: Development of industrial scale PVC nanocomposites with comprehensive enhancement in dielectric properties. IET Sci. Meas. Technol. 13(1), 90–96 (2019)
28. Madonna, V., Giangrande, P., Zhao, W., Buticchi, G., Zhang, H., Gerada, C., Galea, M.: Reliability vs. performances of electrical machines: Partial discharges issue. In: IEEE Workshop on Electrical Machines Design, Control and Diagnosis (WEMDCD) (2019)
29. Madonna, V., Giangrande, P., Zhao, W., Zhang, H., Gerada, C., Galea, M.: On the design of partial discharge-free low voltage electrical machines. In: IEEE International Electric Machines & Drives Conference (IEMDC) (2019)
30. Dunbar, W.G., Seabrook, J.W., High Voltage Design Guide for Airborne Equipment. (BOEING AEROSPACE CO SEATTLE WA, 1976)

How to cite this article: Ji, Y., Giangrande, P., Zhao, W., Madonna, V., Zhang, H., Li, J., Galea, M.: Investigation on combined effect of humidity–temperature on partial discharge through dielectric performance evaluation. IET Sci. Meas. Technol. 1–10 (2022). https://doi.org/10.1049/smt2.12128